Modulation of PI-Specific Phospholipase C by Membrane Curvature and Molecular Order†

Hasna Ahyayauch, Ana V. Villar, Alicia Alonso, and Félix M. Goñi*

Unidad de Biofísica (Centro Mixto CSIC-UPV/EHU) and Departamento de Bioquímica, Universidad del País Vasco, P.O. Box 644, 48080 Bilbao, Spain

Received April 19, 2005; Revised Manuscript Received June 1, 2005

ABSTRACT: Phosphatidylinositol-specific phospholipase C (PI-PLC) from *Bacillus cereus* has been assayed on large and small unilamellar vesicles consisting of PI, either pure or in mixtures with other lipids. Vesicle diameter (in the 50−300 nm range) influences PI-PLC activity, enzyme rates increasing with decreasing curvature radii. With sonicated unilamellar vesicles of pure PI, two apparent K_s values are observed, one in the 0−2 mM concentration range and the other in the 2−12 mM concentration range. The latter (≈4.2 mM) corresponds to previously published values, while the low-concentration K_s is on the same order of magnitude as the single apparent K_m value found with large unilamellar liposomes (≈0.30 mM). PI-PLC appears to be very sensitive to bilayer composition. Certain nonsubstrate lipids, e.g., galactosylceramide or cholesterol, inhibit PI-PLC in a dose-dependent way, at least up to 33 mol % in the bilayers, under conditions with a constant PI concentration. Simultaneous measurements of enzyme activity, interfacial enzyme binding, and fluorescence of different probes, on a variety of bilayer compositions, reveal that both the level of enzyme binding and activity decrease with increasing lipid order, as measured by the fluorescence polarization of the hydrophobic probe diphenylhexatriene. In contrast, no correlation is found for enzyme activity with fluorescence changes of probes, e.g., laurdan, that report on phenomena occurring mainly at the lipid−water interface. Sphingomyelin has a dual effect. Up to 40 mol %, it increases PI-PLC activity, with little effect on bilayer molecular order. At higher proportions, the increased lipid chain order causes a decrease in enzyme activity. The same effects are observed for distearoylphosphatidylcholine when added to PI bilayers. These results support the "two-stage model" for binding of PI-PLC to lipid bilayers, and underline the significance of the enzyme partial penetration into the membrane hydrophobic matrix for its catalytic activity.

Soluble lipases are particularly interesting enzymes from the point of view of biophysical chemistry, because they act on substrates in the solid state, and must therefore transfer themselves from the solution to the solid phase to perform their catalytic activity. Phospholipases C are also of special interest from the biological point of view, because some of their end products (inositol phosphates and diacylglycerol) are potent intracellular signal molecules (*1*−*4*). Phosphatidylinositol-specific phospholipases C (PI-PLCs)[1] of bacterial origin are interesting objects of study, because they exhibit structural and mechanistic similarities with their mammalian counterparts, while being more easily available and structurally simpler. In recent years, a number of important breakthroughs have occurred in the field of bacterial PI-PLCs, chief among them the elucidation of the crystal structure of a *Bacillus* enzyme (*5*, *6*), the mechanistic studies by Tsai, Bruzik, and co-workers (*7*, *8*) and Roberts and co-workers (*9*, *10*), and the studies on the enzyme interaction with nonsubstrate phospholipids, particularly PC, in micelles and vesicles (*11*−*15*).

An aspect of PI-PLC that has not received much attention until recently is the enzyme binding to the membrane bilayer. Peripheral protein binding to lipid interfaces is often analyzed in terms of a two-stage model (*16*, *17*), according to which the protein would first bind the bilayer surface through electrostatic forces, and then form a tight membrane−protein complex stabilized by hydrophobic forces. Wehbi et al. (*18*) have investigated the interfacial binding of PI-PLC from *Bacillus thuringiensis* (whose sequence is very similar to that of the *Bacillus cereus* homologue enzyme) and concluded that its binding behavior is consistent with a two-stage binding model. Also relevant in this context is the observation that, in common with other membrane proteins, PI-PLC contains two Trp residues (Trp47 and Trp242 for the *B. thuringiensis* enzyme) that have a role in lipid binding (*19*). Volwerk et al. (*35*) observed a correlation between PI-PLC

† This work was supported in part by the Spanish Ministerio de Educación y Ciencia (Grants BMC 2002-00784 to A.A. and BFU 2004-02955 to F.M.G.) and by the University of the Basque Country (Grant 9/UPV 00042.310-13552/2001).

* To whom correspondence should be addressed. Phone: +34-94-601 26 25. Fax: +34-94-601 33 60. E-mail: gbpgourf@lg.ehu.es.

[1] Abbreviations: ANTS, 8-aminonaphthalene-1,3,6-trisulfonic acid; Ch, cholesterol; DEPE, dielaidoylphosphatidylethanolamine; DPH, diphenylhexatriene; DPX, *p*-xylenebis(pyridinium bromide); GalCer, pig brain galactosylceramide; GP_{EX}, laurdan-generalized polarization, excitation spectra; laurdan, 6-dodecanoyl-2-(dimethylamino)naphthalene; LUV, large unilamellar vesicle(s); PC, phosphatidylcholine; PE, phosphatidylethanolamine; PI, phosphatidylinositol; PI-PLC, phosphatidylinositol-specific phospholipase C; SD, standard deviation; SEM, standard error of the mean; SUV, small unilamellar vesicle(s); TMA-DPH, 1-(4-trimethylammoniumphenyl)-6-phenyl-1,3,5-hexatriene *p*-toluenesulfate.

10.1021/bi050715k CCC: $30.25
Published on Web 08/04/2005

binding to the phospholipid−water interface, changes in Trp fluorescence emission, and catalytic activity.

This study is intended to explore in further detail the activity of bacterial PI-PLC on PI-containing bilayers, particularly the effects of bilayer composition and curvature on enzyme activity. Unfortunately, the physical properties of PI-based bilayers have not been studied in detail, apart from the early study by Gulik-Krzywicki et al. (*20*) demonstrating the capacity of PI to form lamellar phases when dispersed in water. Also relevant in this respect are the results of Ohki et al. (*21*), who mimicked the effects of phospholipase C on PI bilayers by studying the properties of PI/DAG mixtures. In our experiments, large unilamellar vesicles obtained by extrusion have been used in most cases, although vesicles obtained by sonication have been studied occasionally. The various preparation methods provide vesicles with different radii of curvature, so the effect of this parameter on the PI-PLC activity can be explored. The semisynthetic vesicles offer, in addition, ample possibilities for varying the composition of the lipid bilayers. Our results demonstrate the high sensitivity of bacterial PI-PLC to changes in bilayer composition and curvature, and underline the role of the membrane hydrophobic matrix in the catalytic activity of this otherwise soluble protein.

MATERIALS AND METHODS

Materials. Wheat germ phosphatidylinositol (PI), egg phosphatidylcholine (PC), and egg phosphatidylethanolamine (PE) were purchased from Lipid Products (South Nutfield, United Kingdom). Egg sphingomyelin, pig brain galactosylceramide (GalCer), dielaidoylphosphatidylethanolamine (DEPE), dimyristoylphosphatidylcholine (DMPC), dipalmitoylphosphatidylcholine (DPPC), and distearoylphosphatidylcholine (DSPC) were obtained from Avanti Polar Lipids (Alabaster, AL). Cholesterol and bovine serum albumin (essentially free from fatty acids) were from Sigma. PI-PLC (EC 3.1.4.10) from *B. cereus* was supplied by Molecular Probes Inc. (Eugene, OR). Its purity was checked by SDS−PAGE, with which a single band could be detected after silver staining. Enzyme preparations contained on average 2800 units/mg of protein. 8-Aminonaphthalene-1,3,6-trisulfonic acid (ANTS), *p*-xylenebis(pyridinium bromide) (DPX) diphenylhexatriene (DPH), 1-(4-trimethylammoniumphenyl)-6-phenyl-1,3,5-hexatriene *p*-toluenesulfamate (TMA-DPH), and 6-dodecanoyl-2-dimethylaminonaphthalene (laurdan) were also supplied by Molecular Probes Inc.

Liposome Preparation. Large unilamellar vesicles (LUV) were prepared by the extrusion method using Nuclepore filters (Costar, Cambridge, MA) (0.1 μm pore diameter unless otherwise stated) at room temperature, as detailed previously (*22*, *23*). Small vesicles were prepared by probe sonication as described by Alonso et al. (*24*). All vesicles were prepared in 10 mM Hepes and 50 mM NaCl (pH 7.5). Vesicle size was estimated by quasi-elastic light scattering using a Malvern Zeta-sizer instrument. LUV had average diameters of 103−127 nm, depending on composition, with polydispersity indexes ranging between 0.06 and 0.10. SUV of PI had an average diameter of 48 nm, and a polydispersity index of 0.27. LUV composed of pure PI were also examined by cryo-transmission electron microscopy. The images looked similar to those published by Wehbi et al. (*10*); for a similar system, the average vesicle diameter was, according to this method, 87 ± 10 nm (n = 20).

Enzyme Activity Assays. The PI concentration was 0.3 mM in all experiments, unless otherwise stated. For optimal catalytic activity, the enzyme was assayed at 39 °C, in 10 mM Hepes and 50 mM NaCl (pH 7.5), in the presence of 0.1% bovine serum albumin with continuous stirring. Enzyme was used at a final concentration of 0.16 unit/mL, equivalent to 57 ng of protein/mL. The total volume in the enzyme assays was 1.0 mL. Enzyme activity was assayed by determining water-soluble phosphorus according to Böttcher et al. (*19*). Aliquots (50 μL) were removed from the reaction mixture at regular intervals and extracted with 250 μL of a chloroform/methanol/hydrochloric acid mixture (200/100/1, by volume), and the aqueous phase was assayed for phosphorus. Kinetic data were computed using Enzfit (Elsevier, Biosoft).

Fluorescence Assays for Vesicle Content Leakage. Liposome content leakage was detected using the ANTS/DPX fluorescent probe system described by Ellens et al. (*20*). The assay was performed in a Shimadzu RF-540 spectrofluorophotometer at 39 °C with continuous stirring.

Fluorescence Polarization Assays. The fluorescence polarization of DPH and TMA-DPH was measured at 39 °C, using an SLM 8100 spectrofluorometer, equipped with standard polarization accessories and a circulating water bath. The excitation and emission wavelengths were 360 and 430 nm, respectively, for DPH and 365 and 427 nm, respectively, for TMA-DPH.

The fluorescence polarization was calculated as

$$P = (I_{vv} - GI_{vh})/(I_{vv} + GI_{vh})$$

where I_{vv} and I_{vh} represent the intensity of vertically and horizontally polarized fluorescent light, respectively, when excitation light is vertically polarized. The correction factor $G = I_{hv}/I_{hh}$. I_{hv} and I_{hh} represent the intensity of vertically and horizontally polarized fluorescent light, respectively, when excitation light is horizontally polarized. Fluorescent probes DPH and TMA-DPH were added to the phospholipid to obtain a probe/lipid molar ratio of 1/250.

The generalized polarization (GP) of laurdan was measured with the same equipment mentioned above. The excitation GP_{EX} parameter was calculated according to

$$GP_{EX} = (I_{440} - I_{490})/(I_{440} + I_{490})$$

where I_{440} and I_{490} are the intensities at each excitation wavelength from 325 to 410 nm obtained using fixed emission wavelengths of 440 and 490 nm, respectively. The final probe/lipid molar ratio was 1/1000.

Intrinsic Fluorescence Assay of Interfacial Enzyme Binding. The intrinsic fluorescence spectra of PI-PLC either alone or in the presence of vesicles, but always in the absence of bovine serum albumin, were recorded in an SLM Aminco spectrofluorimeter equipped with a thermostated cell holder and a magnetic stirrer. Small aliquots of a concentrated LUV suspension were added to a fixed concentration of enzyme solution (20 nM) in a cuvette with continuous stirring, exciting the samples at 295 nm and collecting emission between 300 and 420 nm. The slit widths were 5 nm for both excitation and emission. In some experiments, a fixed

lipid concentration was used (134 μM), and the change in fluorescence emission was measured after 1 min. In other cases, the intrinsic fluorescence of PI-PLC was titrated with increasing amounts of lipid, added at 1.5 min intervals.

Spectra were corrected for the light scattered by the LUVs of identical composition and concentration, but in the absence of protein. The signal was also corrected for dilution and inner filter effects as described by White et al. (*42*) using the soluble Trp analogue, NATA, which does not partition into membranes. The apparent mole fraction partition coefficients, $K_{x(app)}$, were determined by fitting the experimental values to the hyperbolic function

$$F/F_0 = 1 + \frac{(F_{max}/F_0 - 1)[L]}{K + [L]}$$

where [L] is the lipid concentration and K is the lipid concentration at which the bound peptide fraction is 0.5. Therefore, $K_{x(app)} = [W]/K$, where [W] is the molar concentration of water.

The fraction of PI-PLC bound to the membranes was estimated according to the equation

$$f_{bound} = K_{x(app)}[L]/([W] + K_{x(app)}[L]) \times 100$$

Direct Assay of Interfacial Enzyme Binding. The phospholipid vesicles were incubated with PI-PLC (0.13 μM) for 30 min at 39 °C, in the absence of bovine serum albumin. Samples were then applied to an Amicon-Centricon-100 filter (100 kDa molecular mass cutoff) and centrifuged at 4 °C and 6100 rpm. This process allows low-molecular weight components (such as free unbound PI-PLC molecules) to filter through (the filtrate), while retaining high-molecular weight components (such as PI-PLC molecules associated with LUVs) atop the filter (the retentate). Fractions of the retentate and filtrate were analyzed by SDS−PAGE with a polyacrylamide gel (15%). The bands were visualized by silver staining (Bio-Rad). The gels stained with silver were scanned with a GS-800 calibrated densitometer (Bio-Rad) and processed with Quantity-One 4.4 (Bio-Rad).

RESULTS

Pure PI Liposomes. PI-specific phospholipase C activity on large unilamellar vesicles consisting of pure PI is shown in Figure 1. The amount of product increases linearly with time in the first 15 min for lipid concentrations between 0.05 and 1.5 mM, when the enzyme concentration is 0.16 unit/mL and the other conditions are as detailed in Materials and Methods. Representative results are shown in Figure 1A. For this range of substrate concentrations, the following apparent kinetic parameters can be obtained: $K_{M-app} = 0.30$ mM and $V_{max-app} = 15$ nmol/min. A longer time course is shown in Figure 1B for 0.3 mM PI, the standard lipid concentration used throughout this study. At the end of 4 h, approximately one-third of the substrate remains intact. Independent experiments show, however, that a 4 h incubation of the enzyme at 39 °C does not alter significantly its specific activity. Vesicle size, initially ≈100 nm, does not vary after 4 h of enzyme treatment during which some two-thirds of the original PI has been converted into diacylglycerol, showing a remarkable stability of the PI-based bilayers (Figure 1B). Metastable giant vesicles containing large amounts of DAG

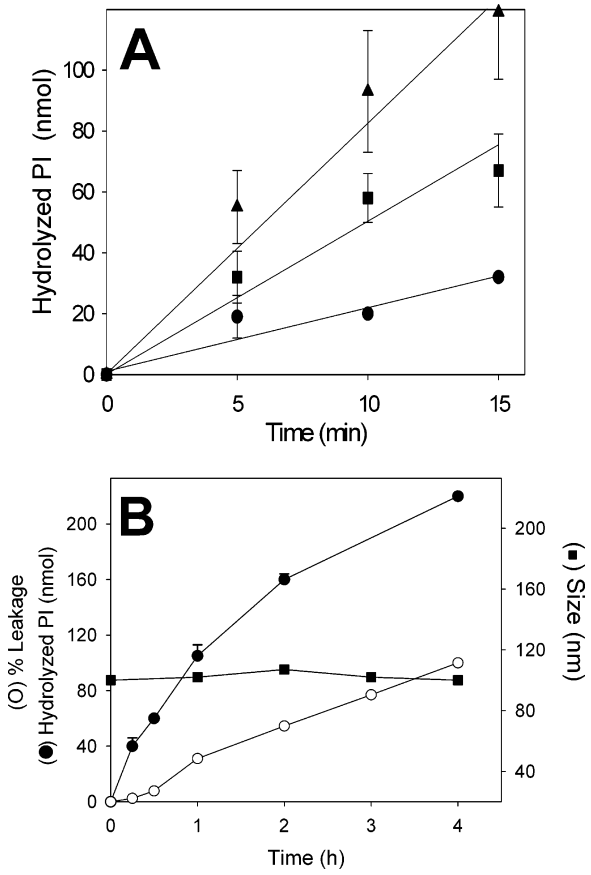

FIGURE 1: PI-PLC activity on large unilamellar vesicles of pure PI. (A) Time course of PI hydrolysis at PI concentrations of (●) 0.075, (■) 0.150, and (▲) 1.200 mM. (B) Long-term kinetics of PI hydrolysis: (●) amount of hydrolyzed PI, (■) vesicle size, and (○) vesicle leakage. The PI concentration was 0.30 mM. In all cases, the enzyme concentration was 0.16 unit/mL. Average values ± SD ($n = 3$).

as a result of phospholipase C activity have been observed recently (*25*). Under our conditions, no changes in vesicle suspension turbidity, indicative of vesicle aggregation, are detected, in agreement with previous observations (*26*). In the course of enzyme action, however, extensive leakage of liposomal contents occurs (Figure 1B). Latency periods (lag times), which are frequently found with many lipases, were not observed in our studies with PI-PLC, either when the substrate was pure PI or in binary mixtures (discussed below) of PI and other lipids.

Effect of Bilayer Curvature. Vesicles of different sizes, in the 50−300 nm range, were prepared using extrusion or sonication procedures, to explore the effect of bilayer curvature on PI-PLC activity. No detergent was included in any of the preparations. The PI concentration was constant at 0.3 mM. The results (Figure 2) show that the rate of PI hydrolysis is clearly influenced by vesicle size, decreasing with increasing radii of curvature. Samples containing PC [Figure 2 (●)] support higher activities (see below), but they still show the inhibitory effect of increasing vesicle diameters.

A more detailed comparison of LUV (ca. 100 nm) and SUV (ca. 50 nm) consisting of pure PI was carried out by studying the enzyme kinetics for both kinds of vesicles in the 0−12 mM concentration range (Figure 3). The difference in activity between SUV and LUV is particularly clear at lipid concentrations above 2 mM. Even more significant is

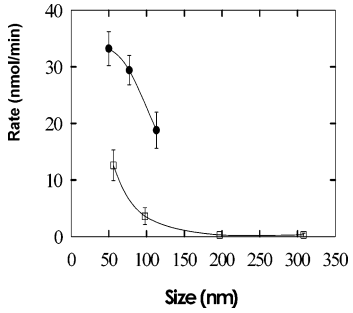

FIGURE 2: Dependence of PI-PLC activity on vesicle size. Vesicle composition was pure PI (□) or PI and PC (2/1 molar ratio) (●). Average values ± SEM ($n = 3$). The smaller (50 nm) vesicles were prepared by sonication, and their polydispersity was 0.27 ± 0.1. Larger vesicles were obtained by extrusion, and their polydispersities were in the range of 0.06−0.10.

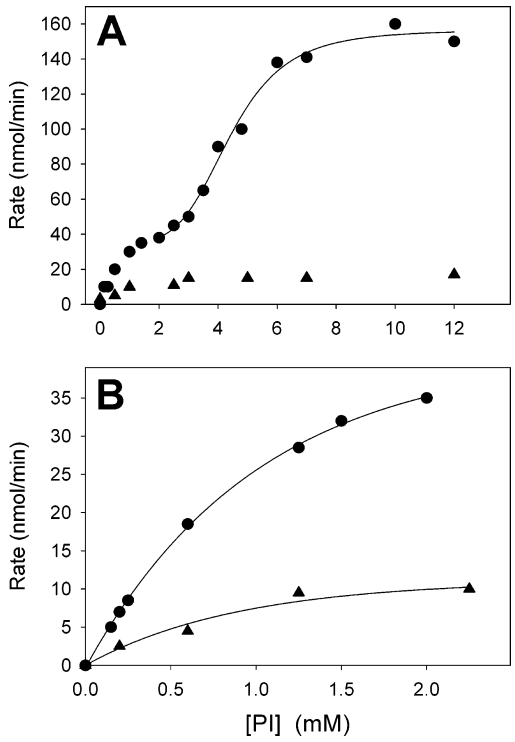

FIGURE 3: Effect of bilayer curvature on PI-PLC activity as assayed on pure PI bilayers. (A) Activity vs PI concentration for the substrate in the form of (●) SUV or (▲) LUV. The curve drawn for SUV at PI concentrations above 2 mM corresponds to a cooperative kinetics with an apparent K_s of 4.2 mM. (B) A detailed plot of the portion of the above figure for PI concentrations below 2 mM. The curves correspond to Michaelian hyperbolas with apparent K_m values of 0.30 (LUV) and 0.77 mM (SUV).

the fact that the shape of the velocity versus substrate concentration plots is different in SUV and LUV. In the latter case, the data fit a Michaelian hyperbola with a K_{M-app} of 0.30 mM and a $V_{max-app}$ of 15 nmol/min, as mentioned at the beginning of the Results. The behavior of SUV is more complex. Qian et al. (*15*) had already observed the non-Michaelian nature of this kinetics. By studying a large number of PI concentrations in the 0−3 mM concentration range (Figure 3B), we detected two apparent K_s values, ~0.77 and 4.2 mM for low and high lipid concentrations, respectively. In addition, cooperative kinetics is observed at PI concentrations above 2 mM for SUV. At low SUV concentrations, the observed K_s is on the same order of magnitude as the K_{M-app} measured with LUV, while the high-SUV concentration K_s is very similar to the one described by Qian et al. (*15*) (2.6 ± 0.5 mM), although under our conditions the absolute values of enzyme rates are higher. The apparent K_s values obtained under these conditions are difficult to analyze, because they contain contributions from both interfacial affinity and active site affinity (*15*). The two observed K_s values may correspond to two modes of enzyme docking to the SUV membrane, of which only one would exist in LUV. It could be suggested, as a hypothesis, that SUV offer, in addition to the "regular" bilayer surface, a number of edges and/or defects that would provide, at higher vesicle concentrations, a significant second site for enzyme binding. These inhomogeneities would be absent in the smoother, less strained LUV. Because of the irregular nature of these high-K_s binding sites, the arrival of an enzyme molecule would cause a local rearrangement of the surrounding molecules, and this in turn could be at the origin of the observed cooperativity in SUV. No such short-distance effects would be expected in the more homogeneous LUV.

PI in Mixed Bilayers. To examine the sensitivity of PI-PLC to lipids other than its substrate in the membrane, a series of bilayer compositions, containing PI and an additional lipid, were tested as PI-PLC substrates. Enzyme activities for a number of binary mixtures in which PI and the nonsubstrate lipid were present at a 2/1 molar ratio are collected in Table 1. PC and to a lesser extent SM enhance the enzyme activity of the enzyme, and PE has no clear effect; DEPE, Ch, and GalCer inhibit PI-PLC. All the experiments shown in Table 1 have been performed at a constant PI concentration of 0.3 mM. However, for some lipid compositions, enzyme activities were assayed at 4 mM PI, i.e., well above the K_M. The same trends in activatory and inhibitory effects were observed. The measured activities at 4 mM PI were for pure PI LUV, 10.8 ± 2.1 nmol/min, for PI and egg PC, 38.0 ± 2.7 nmol/min, for PI and Ch, 2.4 ± 0.6 nmol/min, and for PI and GalCer, 1.5 ± 0.8 nmol/min (average values ± standard deviation, $n = 3$). The corresponding relative activities, as compared to that of pure PI, are 3.6, 1.0, 0.22, and 0.13, respectively, similar to those given in Table 1 for a substrate concentration of 0.3 mM. PE, SM, and PC had already been tested by Qian et al. (*15*) on SUV. The relative changes in enzyme activity were virtually the same as those measured by us on LUV. The effect of PC is particularly noteworthy, and is due to this phospholipid acting as an allosteric activator of PI-PLC (*14*). The inhibitory effects of Ch, DEPE, and GalCer have not been reported previously, and will be further discussed below.

The activating and inhibiting effects of PC and Ch, respectively, were studied in more detail at a constant PI concentration (Figures 4 and 5). In parallel with enzyme activity, changes in "generalised polarisation" of laurdan fluorescence excitation spectra GP_{EX} (*27*) and in polarization of DPH and TMA-DPH fluorescence (*28*, *29*) were recorded for all the lipid mixtures that were studied. PC (Figure 4) increases enzyme activity in a dose-dependent way for molar fractions in the 0.05−0.35 range (Figure 4A). The levels of laurdan GP_{EX} (Figure 4B) and TMA-DPH polarization (Figure 4D) decrease gradually as mirror images of the increase in enzyme rate. DPH polarization, in turn (Figure 4C), changes significantly only at 33 mol % PC. The effects of cholesterol are very different (Figure 5). Enzyme activity decreases with Ch in a dose-dependent way (Figure 5A),

Table 1: PI-PLC Activity on Large Unilamellar Vesicles of Varying Lipid Compositions, and Their Physical Properties As Detected by Fluorescence Probes[a]

lipid composition (molar ratios)	enzyme activity (nmol of PI cleaved/min)	relative activity	laurdan GP_{EX}	DPH polarization	TMA-DPM polarization
2/1 PI/egg PC	26.5 ± 1.8	7.0	−0.08 ± 0.003	0.115 ± 0.013	0.175 ± 0.03
2/1 PI/SM	7.3 ± 1.5	1.9	−0.035 ± 0.006	0.123 ± 0.004	0.290 ± 0.010
pure PI	3.8 ± 0.3	1.0	0.025 ± 0.0150	0.129 ± 0.017	0.272 ± 0.023
2/1 PI/PE	3.5 ± 0.8	0.92	−0.031 ± 0.005	0.129 ± 0.005	0.291 ± 0.015
2/1 PI/DEPE	2.2 ± 0.4	0.58	−0.064 ± 0.012	0.136 ± 0.004	0.279 ± 0.003
2/1 PI/Ch	1.2 ± 0.3	0.31	0.25 ± 0.01	0.198 ± 0.006	0.298 ± 0.012
2/1 PI/GalCer	0.5 ± 0.1	0.13	−0.037 ± 0.009	0.191 ± 0.010	0.297 ± 0.011

[a] The PI concentration was constant at 0.3 mM. The enzyme concentration was 57 ng/mL. The values that are given correspond to average values ± SEM ($n = 3$).

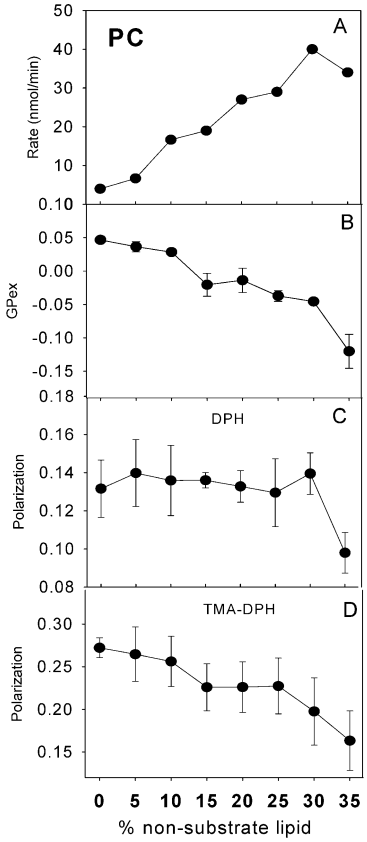

FIGURE 4: Effect of increasing amounts of PC in PI LUV bilayers on PI-PLC activity and membrane physical properties: (A) enzyme activity, (B) laurdan GP_{EX}, (C) DPH fluorescence polarization, and (D) TMA-DPH fluorescence polarization. Data in panel A are averages of two closely similar measurements. In panels B−D, data are average values ± SD ($n = 3$).

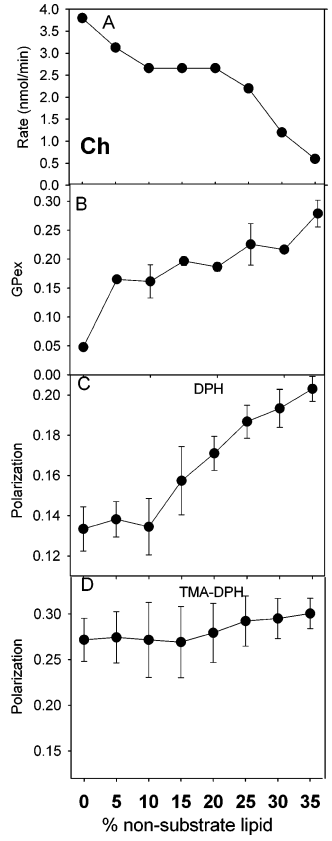

FIGURE 5: Effect of increasing amounts of Ch in PI LUV bilayers on PI-PLC activity and membrane physical properties: (A) enzyme activity, (B) laurdan GP_{EX}, (C) DPH fluorescence polarization, and (D) TMA-DPH fluorescence polarization. Data in panel A are averages of two closely similar measurements. In panels B−D, data are average values ± SD ($n = 3$).

while the sterol causes gradual increases in the level of laurdan GP_{EX} (Figure 5B), and DPH polarization (Figure 5C), with no significant changes in TMA-DPH polarization (Figure 5D).

In an effort to detect and rationalize any putative relationship between enzyme activity and changes in the physical properties of the bilayer, laurdan GP_{EX}, DPH, and TMA-DPH fluorescence polarization were recorded for all the lipid mixtures mentioned in Table 1. No correlation that could be extended to all lipid mixtures was found between changes in enzyme activity and changes in laurdan GP_{EX} or TMA-DPM polarization. However, an inverse relationship appears to exist between enzyme activation and DPH fluorescence polarization. The latter parameter is usually interpreted as a measure of molecular order in bilayers (*28*, *30*). Thus, from the data in Table 1, enzyme activity appears to be enhanced when the lipid bilayer becomes more disordered.

In view of these data, enzyme activities and DPH polarization values were recorded for a series of lipid mixtures, in addition to those mentioned in Table 1. A plot of enzyme activities versus DPH polarization values for all the samples is presented in Figure 6. PI-PLC activity decreases nonlinearly with DPH polarization, i.e., with an increase in lipid order.

Effect of Choline-Containing Phospholipids. The effects of SM were studied in more detail. The data in Table 1 show an increased PI-PLC activity and, correspondingly, a small decrease in DPH polarization. However, pure egg SM has a very high gel-to-fluid transition temperature, of ca. 40 °C (*31*); thus, it is expected to decrease membrane fluidity

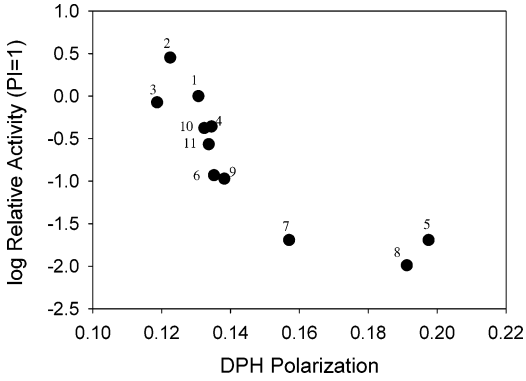

FIGURE 6: Relationship between PI-PLC activity and bilayer molecular order. Enzyme activity values are relative to the activity on pure PI bilayers. Average values of three independent measurements. Bilayer compositions are (in molar ratios) as follows: 1, pure PI; 2, 2/1 PI/SM; 3, 2/1 PI/PE; 4, 9/1 PI/Ch; 5, 2/1 PI/Ch; 6, 9/1 PI/GalCer; 7, 8/2 PI/GalCer; 8, 2/1 PI/GalCer; 9, 9/1 PI/DEPE; 10, 8/2 PI/DEPE; and 11, 2/1 PI/DEPE.

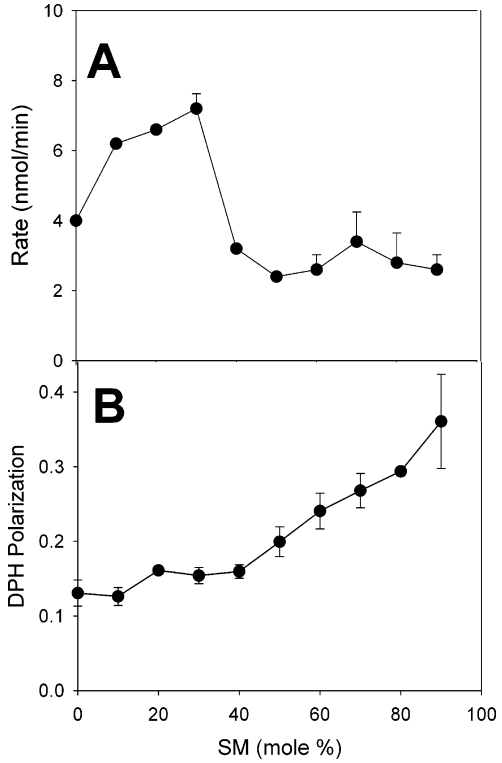

FIGURE 7: Effect of increasing amounts of SM in PI LUV bilayers on PI-PLC activity and DPH polarization: (A) enzyme activity and (B) DPH fluorescence polarization. Data are average values ± SD ($n = 3$).

beyond a certain concentration in the bilayer. PI/SM mixtures containing between 10 and 90 mol % SM were prepared. The corresponding enzyme activities (at a constant PI concentration of 0.3 mM) and DPH polarization values are shown in Figure 7. Up to 30 mol % SM, PI-PLC rates are enhanced, despite a minor increase in DPH polarization. Higher SM concentrations cause a clear increase in DPH polarization, and a decreased enzyme activity. This dual behavior of SM is probably due to the simultaneous presence of two opposing effects, namely, SM acting as an enzyme activator, being a structural analogue of PC (*14*), and as an enzyme inhibitor, due to its ordering effect. The former property prevails at ≤30 mol % SM and the latter one above that SM concentration.

The hypothesis of the two opposing effects, i.e., allosteric activation versus lipid ordering-induced inhibition, was further tested with mixtures of PI and one of three saturated PC phospholipids, namely, DMPC, DPPC, and DSPC, whose gel-to-fluid transition temperatures are 23, 41, and 55 °C, respectively. Data of enzyme activities and DPH polarization, all of them recorded at 39 °C, are shown in Figure 8. DMPC and DPPC do not give rise, at that temperature, to major changes in DPH polarization, and PI-PLC activity increases monotonically because of the choline activation effect (Figure 8A,B,D,E). DSPC, however, increases significantly the bilayer molecular order, and a small increase in activity at 40 mol % DSPC is neutralized and effectively inverted at higher DSPC concentrations, when the latter phospholipid is causing a significant increase in DPH polarization (Figure 8C,F). The effect of DSPC is qualitatively similar to that of SM. Note that the PC phospholipid whose transition temperature is similar to that of SM is DPPC, and not DSPC. However, SM is known to have a particular tendency to support ordered conformations in bilayers. The data in Figure 8 do not show the "surface dilution" effect observed for SUV composed of PI and DMPC (*15*). Apart from the different temperatures used in those (30 °C) and these (39 °C) experiments, surface dilution may be less evident in LUV where the enzyme, presumably operating in the scooting mode, would have in any case a large amount of accessible substrate.

Interfacial Binding of PI-PLC. As a further step in our understanding of the PI-PLC interaction with bilayers of mixed lipid compositions, we studied the interfacial binding of the enzyme. Two complementary methods were used, a direct binding assay and a procedure based on surface-induced changes in enzyme intrinsic fluorescence. In both methods, bovine serum albumin, which is customarily added in the enzyme assays, was omitted. This had the 2-fold purpose of facilitating the artifact-free detection of enzyme binding to bilayers, by removing fluorescence emission from albumin, and of lowering the enzyme activity. The latter effect weakens the influence of the enzyme end product diacylglycerol on the binding of enzyme to vesicles. Direct binding was estimated by incubating solutions of PI-PLC with LUV and then filtering the suspensions to separate free PI-PLC from bound PI-PLC (*18*). A control assay in which no vesicles are present is used to measure the efficiency of free enzyme recovery in the process. The results are presented in Figure 9A. Both pure PI and PI/PC bilayers support full binding under these conditions but, more interestingly, enzyme binding to PI/Ch and PI/GalCer bilayers, which allow only a reduced enzyme activity (see Table 1), is also significantly decreased, by 40−45%. No quantitative correlation is observed between the degrees of inhibition of activity and binding, as expected from the different experimental conditions (in particular enzyme concentration and the presence or absence of bovine serum albumin) required in both kinds of assays. However, it can be ascertained that the more ordered bilayers bind less enzyme.

PI-PLC activity assays carried out under the experimental conditions of Figure 9A indicated that, after incubation for 30 min, the proportion of hydrolyzed PI varied from 2% in PI/GalCer bilayers to 14% in PI/PC samples (data not shown). To ensure that the enzyme end product diacylgly-

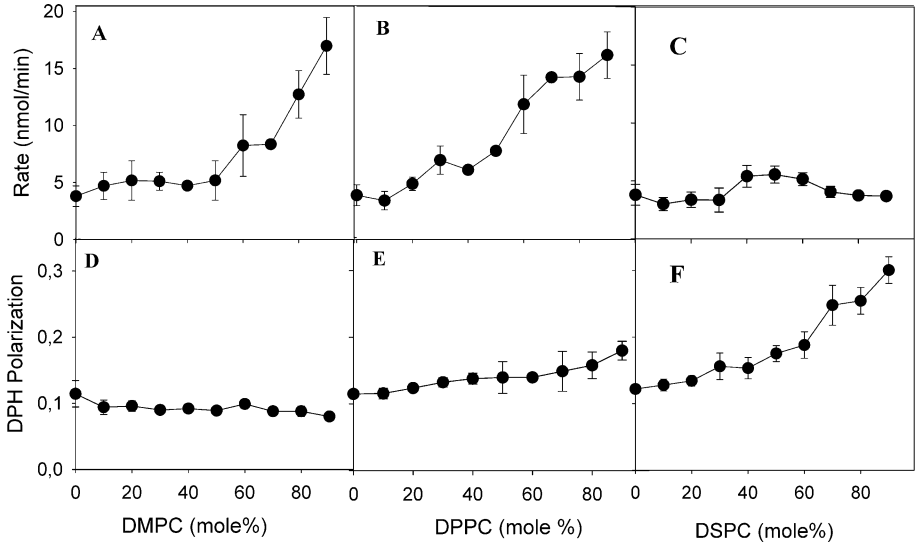

FIGURE 8: Effect of increasing amounts of saturated phosphatidylcholines in PI LUV bilayers on (A−C) PI-PLC activity and (D−F) DPH polarization. The saturated PCs were (A and D) DMPC, (B and E) DPPC, and (C and F) DSPC. Data are average values ± SD ($n = 3$).

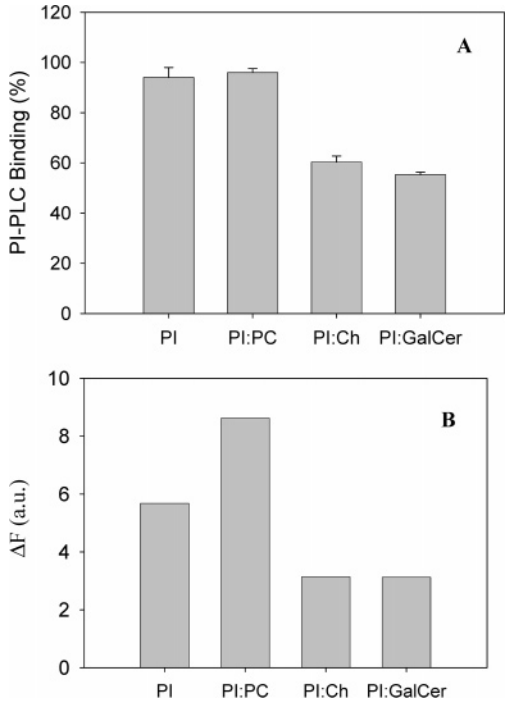

FIGURE 9: Interfacial binding of PI-PLC to LUV. In a direct assay (A), enzyme and vesicles were incubated together, and then vesicle-bound and -free enzyme molecules were separated by filtration (see Materials and Methods); 100% was the sum of free and bound enzyme molecules. Average values ± SD ($n = 3$). In the intrinsic fluorescence assay (B), the effect of liposome composition on the increase in the intrinsic fluorescence of PI-PLC in the first 1 min after addition of vesicles was determined. The lipid concentration used in these experiments was 134 μM. Average values of two closely similar measurements are given.

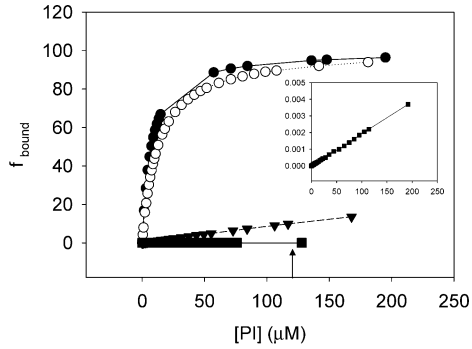

FIGURE 10: Fluorescence titration assay of interfacial enzyme binding. Binding is estimated from the increase in the PI-PLC intrinsic fluorescence. The bilayer composition was (●) pure PI, (○) 2/1 PI/PC, (▼) 2/1 PI/Ch, and (■) 2/1 PI/GalCer. The inset shows data for PI−GalCer binding with an expanded ordinate scale.

cerol was not perturbing our binding measurements, binding was qualitatively assayed in an independent way as the increase in the intrinsic fluorescence of PI-PLC 1 min after liposome addition. The bilayer provides a less polar environment for the Trp residues that are involved, and this in turn increases their fluorescence yield. Under our conditions, no more than 2% of PI is hydrolyzed in any case in the first minute (data not shown). The change in PI-PLC intrinsic fluorescence, corrected for scattering and inner-filter effects, is shown in Figure 9B. The results confirm again that the more ordered bilayers bind less enzyme.

The intrinsic fluorescence of PI-PLC can be titrated with increasing amounts of PI-containing vesicles, as in Figure 10. The results in this figure are normalized to an arbitrary value of 100, attributed to the largest observed increase in fluorescence intensity, in this case with PI/PC vesicles. The vertical arrow near 134 μM PI indicates the conditions under which direct binding and intrinsic fluorescence data were collected (Figure 9). In agreement with the direct binding data, both PI and PI/PC bilayers allow a similar extent of enzyme binding. However, the increase in fluorescence that accompanies binding to PI/Ch or PI/GalCer membranes is much smaller than expected from the observed degrees of direct binding (Figure 9A) or enzyme activity (Table 1). It should be noted in this respect that fluorescence changes alone may be misleading for a quantitative assessment of enzyme binding to membranes, although again the data in Figures 9B and 10 provide qualitative information about the lower extent of enzyme binding to bilayers containing more ordered lipids.

DISCUSSION

PI-PLC belongs to the extensive group of proteins that are not found in a stable membrane-bound form under

physiological conditions, yet they must interact with the membrane to perform their specific function. They have been denoted as "non-permanent membrane proteins" (*32*). As mentioned in the introductory section, PI-PLC has been proposed (*18*) to bind the membrane bilayer following the two-stage model for peripheral protein binding to lipid interfaces (*16*, *17*), according to which a first step, dominated by electrostatic interactions, would be followed by a second stage, governed by predominantly hydrophobic forces, firmly securing the protein to the bilayer lipids. The results in this paper demonstrate that PI-PLC activity is enhanced by high vesicle curvature and by low molecular order in the bilayer. We propose that both these factors will affect enzyme activity through facilitation of the second stage of binding, i.e., the hydrophobic interactions.

In their study on the interfacial binding of PI-PLC, Wehbi et al. (*18*) found that the enzyme binds with much higher affinity SUV than LUV of a given composition. Our data in Figure 2 demonstrate a correlation between decreased curvature and decreased activity when going from SUV to larger vesicles. The combined data of Wehbi et al. and our own strongly suggest that curvature, binding, and catalytic activity are closely linked in the operation of PI-PLC. Both for pure PI and for PI/PC vesicles, enzyme rates decrease rapidly with diameters increasing from ≈50 to 100 nm. Further increases in diameter lead to a slower fall in activities. It should be noted in this respect that 50 nm vesicles, obtained by sonication, are metastable, with phospholipid molecules in the outer monolayer covering a maximum area per molecule, and prone to destabilization by other amphiphiles (*33*). Vesicles with diameters of ≥100 nm, however, are stable for all practical purposes, their properties being very similar to those of bilayers in cell membranes. Consistent with the idea that PLCs must do work in penetrating monolayers (*34*), the maximally spread phospholipids in the outer monolayer of sonicated vesicles may allow an easier access of the already electrostatically bound enzyme to the fatty acyl chains. The cooperative kinetics found in SUV, but not in LUV (Figure 3), also reflects a different form of interaction of PI-PLC with the smaller vesicles, as suggested above.

The sensitivity of PI-PLC to the presence of phospholipids other than its substrate has been the object of several studies in the past (*14*, *15*, *35*, *36*). The LUV system provides a good opportunity to explore this property of the enzyme. The data in Table 1 and Figures 4−6 indicate a positive correlation of enzyme activity with lipid chain disorder. The three fluorescent probes used were selected to provide different kinds of information about the physical state of the bilayer. Laurdan is an amphiphilic probe that orients in parallel with the acyl chains, the fluorophore being located close to the membrane surface. The excited-state relaxation of laurdan is determined by the presence and mobility of water molecules within the lipid bilayer, an increase in GP_{EX} indicating a reduction in the number of interactions between laurdan and water molecules (*27*, *37*). DPH and TMA-DPH molecules have a cylinder shape, with fluorescence excitation and emission dipoles approximately parallel to their long axis. Consequently, their fluorescence polarization is very sensitive to reorientation of the probe long axis as a result of interactions with surrounding molecules (*38*). Thus, DPH fluorescence polarization is frequently used to monitor changes in membrane molecular order (*28*, *30*). DPH fluorescence polarization reports on the membrane physical state mainly through changes in angular reorientation of lipid acyl chains (*28*, *38*). The main difference between DPH and TMA-DPH is their location in the bilayers. DPH resides within the hydrophobic membrane matrix, either parallel to the fatty acyl chains or parallel to the membrane plane, but in the center of the bilayer. The trimethylammonium group of TMA-DPH acts as a surface anchor so that the latter probe reports on changes taking place close to the lipid−water interface (*29*, *36*).

Enzyme binding measured under the experimental conditions in Figure 9A reflects mainly the second stage of binding, since the initial electrostatic vesicle interaction alone would not be detected after the filtering and washing steps. Thus, there is a good (though not quantitative, for the reasons given above) correlation between increased lipid order, a decreased level of hydrophobic (second step) binding, and decreased hydrolytic activity. The fluorescence data in Figures 9B and 10 are interesting in this respect. *B. cereus* PI-PLC consists of a distorted $(\beta\alpha)_6$ barrel (*5*). It has been well established that interfacial binding of the enzyme to phospholipid interfaces involves a region at the top of the barrel rim containing two Trp exposed to solvent, Trp-47 in helix β and Trp-242 in the flexible loop of residues 232−244 (*12*, *13*, *19*). Of these, Trp-47 appears to be disposed in a more water-accessible region of the bilayer when membrane-bound, while Trp-242 would penetrate further into the lipid layer, perhaps because of the flexibility of the loop region (*19*). Also relevant in this context is the observation that Trp-242 is responsible for most of the increase in intrinsic fluorescence when PI-PLC binds micelles (*19*). In view of these data, and of the observations in this paper, it can be suggested that the decreased level of enzyme binding (due to a higher lipid order) is mainly due to a decreased level of membrane insertion of the loop of residues 232−244, and that such hindered insertion is in turn related to the inhibition of enzyme activity.

Concluding Remarks. The results in this paper show that PI-PLC activity and binding correlate with changes in molecular order taking place within the bilayer hydrophobic matrix, rather than at its surface. These observations, together with the previously observed correlation between PI-PLC binding to the lipid bilayer and its catalytic activity (*18*, *35*), suggest that a decreased membrane lipid order facilitates the hydrophobic interactions (stage 2 of the two-stage model) that lead to insertion of PI-PLC into the bilayer (*18*, *34*) and formation of a catalytically active complex. The importance of hydrophobic interactions in this context has been put forward repeatedly by Roberts and co-workers (*39*−*41*). In addition, changes in molecular order will also have a profound effect on the accessibility of the substrate and removal of diacylglycerol to and from the enzyme active site, particularly considering that the enzyme appears to act in the processive or scooting mode (*35*). Thus, although our results on the effects of both vesicle curvature and lipid order fully support the importance of hydrophobic interactions in PI-PLC binding, further studies will be required to determine the extent to which these factors influence as well the catalytic cycle of the bound enzyme.

REFERENCES

1. Martelli, A. M., Manzoli, L., and Cocco, L. (2004) Nuclear inositides: Facts and perspectives, *Pharmacol. Ther. 101*, 47−64.
2. Nahorski, S. R., Young, K. W., Challiss, R. A. J., and Nash, M. S. (2003) Visualizing phosphoinositide signalling in single neurons gets a green light, *Trends Neurosci. 26*, 444−452.
3. Irvine, R. F. (2003) 20 years of Ins(1,4,5)P3, and 40 years before, *Nat. Rev. Mol. Cell Biol. 4*, 586−590.
4. Roberts, M. F. (1996) Phospholipases: Structural and functional motifs for working at an interface, *FASEB J. 10*, 1159−1172.
5. Heinz, D. W., Ryan, M., Bullock, T. L., and Griffith, O. H. (1995) Crystal structure of the phosphatidylinositol-specific phospholipase C from *Bacillus cereus* in complex with myo-inositol, *EMBO J. 14*, 3855−3863.
6. Ryan, M., Liu, T., Dahlquist, F. W., and Griffith, O. H. (2001) A catalytic diad involved in substrate-assisted catalysis: NMR study of hydrogen bonding and dynamics at the active site of phosphatidylinositol-specific phospholipase C, *Biochemistry 40*, 9743−9750.
7. Hondal, R. J., Zhao, Z., Kravchuk, A. V., Liao, H., Riddle, S. R., Yue, X., Bruzik, K. S., and Tsai, M. D. (1998) Mechanism of phosphatidylinositol-specific phospholipase C: A unified view of the mechanism of catalysis, *Biochemistry 37*, 4568−4580.
8. Kubiak, R. J., Yue, X., Hondal, R. J., Mihai, C., Tsai, M. D., and Bruzik, K. S. (2001) Involvement of the Arg-Asp-His catalytic triad in enzymatic cleavage of the phosphodiester bond, *Biochemistry 40*, 5422−5432.
9. Feng, J., Stieglitz, K., and Roberts, M. F. (2004) Mutation of two active-site residues converts a phosphatidylinositol-specific phospholipase C to a glucose phosphatase, *J. Am. Chem. Soc. 126*, 1008−1009.
10. Wehbi, H., Feng, J., and Roberts, M. F. (2003) Water-miscible organic cosolvents enhance phosphatidylinositol-specific phospholipase C phosphotransferase as well as phosphodiesterase activity, *Biochim. Biophys. Acta 1613*, 15−27.
11. Berg, O. C., Yu, B. Z., Apitz-Castro, R. J., and Jain, M. K. (2004) Phosphatidylinositol-specific phospholipase C forms different complexes with monodisperse and micellar phosphatidylcholine, *Biochemistry 43*, 2080−2090.
12. Zhang, X., Wehbi, H., and Roberts, M. F. (2004) Cross-linking phosphatidylinositol-specific phospholipase C traps two activating phosphatidylcholine molecules on the enzyme, *J. Biol. Chem. 279*, 20490−20500.
13. Feng, J., Bradley, W. D., and Roberts, M. F. (2003) Optimizing the interfacial binding and activity of a bacterial phosphatidylinositol-specific phospholipase C, *J. Biol. Chem. 278*, 24651−24657.
14. Zhou, C., Qian, X., and Roberts, M. F. (1997) Allosteric activation of phosphatidylinositol-specific phospholipase C: Specific phospholipid binding anchors the enzyme to the interface, *Biochemistry 36*, 10089−10097.
15. Qian, X., Zhou, C., and Roberts, M. F. (1998) Phosphatidylcholine activation of bacterial phosphatidylinositol-specific phospholipase C toward PI vesicles, *Biochemistry 37*, 6513−6522.
16. Stahelin, R.-V., and Cho, W. (2001) Differential roles of ionic, aliphatic, and aromatic residues in membrane-protein interactions: A surface plasmon resonance study on phospholipases A2, *Biochemistry 40*, 4672−4678.
17. Wallace, B. A., and Janes, R. W. (1999) Tryptophans in membrane proteins. X-ray crystallographic analyses, *Adv. Exp. Med. Biol. 467*, 789−799.
18. Wehbi, H., Feng, J., Kolbeck, J., Ananthanarayanen, B., Cho, W., and Roberts, M. F. (2003) Investigating the interfacial binding of bacterial phosphatidylinositol-specific phospholipase C, *Biochemistry 42*, 9374−9382.
19. Feng, J., Wehbi, H., and Roberts, M. F. (2002) Role of tryptophan residues in interfacial binding of phosphatidylinositol-specific phospholipase C, *J. Biol. Chem. 277*, 19867−19875.
20. Gulik-Krzywicki, T., Schechter, E., and Luzzati, V. (1969) Interactions of proteins and lipids: Structure and polymorphism of protein-lipid-water phases, *Nature 223*, 1116−1121.
21. Ohki, K., Sekiya, T., Yamauchi, T., and Nozawa, Y. (1982) Effect of phosphatidylinositol replacement by diacylglycerol on various physical properties of artificial membranes with respect to the role of phosphatidylinositol response, *Biochim. Biophys. Acta 693*, 341−350.
22. Basañez, G., Nieva, J. L., Goñi, F. M., and Alonso, A. (1996) Origin of the lag period in the phospholipase C cleavage of phospholipids in membranes. Concomitant vesicle aggregation and enzyme activation, *Biochemistry 35*, 15183−15187.
23. Nieva, J. L., Goñi, F. M., and Alonso, A. (1989) Liposome fusion catalytically induced by phospholipase C, *Biochemistry 28*, 7364−7367.
24. Alonso, A., Saez, R., Villena, A., and Goñi, F. M. (1982) Increase in size of sonicated phospholipid vesicles in the presence of detergents, *J. Membr. Biol. 67*, 55−62.
25. Riske, K. A., and Döbereiner, H. G. (2003) Diacylglycerol-rich domain formation in giant stearoyl-oleoyl phosphatidylcholine vesicles driven by phospholipase C activity, *Biophys. J. 85*, 2351−2362.
26. Villar, A. V., Alonso, A., and Goñi, F. M. (2000) Leaky vesicle fusion induced by phosphatidylinositol-specific phospholipase C: Observation of mixing of vesicular inner monolayers, *Biochemistry 39*, 14012−14018.
27. Bagatolli, L. A., Gratton, E., and Fidelio, G. D. (1998) Water dynamics in glycosphingolipid aggregates studied by LAURDAN fluorescence, *Biophys. J. 75*, 331−341.
28. Lentz, B. R. (1993) Use of fluorescent probes to monitor molecular order and motions within liposome bilayers, *Chem. Phys. Lipids 64*, 99−116.
29. Basañez, G., Nieva, J. L., Rivas, E., Alonso, A., and Goñi, F. M. (1996) Diacylglycerol and the promotion of lamellar-hexagonal and lamellar-isotropic phase transitions in lipids: Implications for membrane fusion, *Biophys. J. 70*, 2299−2306.
30. Mitchell, D. C., and Litman, B. J. (1998) Effect of cholesterol on molecular order and dynamics in highly polyunsaturated phospholipid bilayers, *Biophys. J. 75*, 896−908.
31. Ruiz-Argüello, M. B., Veiga, M. P., Arrondo, J. L. R., Goñi, F. M., and Alonso, A. (2002) Sphingomyelinase cleavage of sphingomyelin in pure and mixed lipid membranes. Influence of the physical state of the sphingolipid, *Chem. Phys. Lipids 114*, 11−20.
32. Goñi, F. M. (2002) Non-permanent proteins in membranes: When proteins come as visitors, *Mol. Membr. Biol. 19*, 237−245.
33. Gershfeld, N. L. (1978) Equilibrium studies of lecithin-cholesterol interactions I. Stoichiometry of lecithin-cholesterol complexes in bulk systems, *Biophys. J. 22*, 469−488.
34. Boguslavsky, V., Rebecchi, M., Morris, A. J., Jhon, D. Y., Rhee, S. G., and McLaughlin, S. (1994) Effect of monolayer surface pressure on the activities of phosphoinositide-specific phospholipase C-β1, -γ1, and -δ1, *Biochemistry 33*, 3032−3037.
35. Volwerk, J. J., Filthuth, E., Griffith, O. H., and Jain, M. K. (1994) Phosphatidylinositol-specific phospholipase C from *Bacillus cereus* at the lipid-water interface: Interfacial binding, catalysis, and activation, *Biochemistry 33*, 3464−3474.
36. Hofmann, S. L., and Majerus, P. W. (1982) Modulation of phosphatidylinositol-specific phospholipase C activity by phospholipid interactions, diglycerides, and calcium ions, *J. Biol. Chem. 257*, 14359−14364.
37. Parasassi, T., De Stasio, G., d'Ubaldo, A., and Gratton, E. (1991) Quantitation of lipid phases in phospholipid vesicles by the generalized polarization of Laurdan fluorescence, *Biophys. J. 60*, 179−189.
38. Haugland, R. P. (2002) *Handbook of Fluorescent Probes and Research Products*, 9th ed., pp 535−540, Molecular Probes Inc., Eugene, OR.
39. Soltys, C. E., Bian, J., and Roberts, M. F. (1993) Polymerizable phosphatidylcholines: Importance of phospholipid motions for optimum phospholipase A2 and C activity, *Biochemistry 32*, 9545−9552.
40. Kobayashi, M., Mutharasan, R. K., Feng, J., Roberts, M. F., and Lomasney, J. W. (2004) Identification of hydrophobic interactions between proteins and lipids: Free fatty acids activate phospholipase Cδ1 via allosterism, *Biochemistry 43*, 7522−7533.
41. Zhang, X., Feng, J., Zambonelli, C., Head, J., Seaton, B., and Roberts, M. F. (2004) Role of helix B residus in membrane binding by a bacterial PI-PLC, *FASEB J. 18*, C186.
42. White, S. H., Wimley, W. C., Ladokhin, A. S., and Hristova, K. (1998) Protein folding in membranes: Determining energetics of peptide-bilayer interactions, *Methods Enzymol. 295*, 62−87.

BI050715K